Front. Eng. Manag. 2017, 4(3): 348–356
DOI 10.15302/J-FEM-2017043

RESEARCH ARTICLE

Zhi LI, Feng QIAN, Wenli DU, Weimin ZHONG

DE based economic control chart design and application for a typical petrochemical process

Abstract Petrochemical industry plays an important role in the development of the national economy. Purified terephthalic acid (PTA) is one of the most important intermediate raw materials in the petrochemical and chemical fiber industries. PTA production has two parts: *p*-xylene (PX) oxidation process and crude terephthalic acid (CTA) hydropurification process. The CTA hydropurification process is used to reduce impurities, such as 4-carboxybenzaldehyde, which is produced by a side reaction in the PX oxidation process and is harmful to the polyester industry. From the safety and economic viewpoints, monitoring this process is necessary. Four main faults of this process are analyzed in this study. The common process monitoring methods always use T^2 and SPE statistic as control limits. However, the traditional methods do not fully consider the economic viewpoint. In this study, a new economic control chart design method based on the differential evolution (DE) algorithm is developed. The DE algorithm transforms the economic control chart design problem to an optimization problem and is an excellent solution to such problem. Case studies of the main faults of the hydropurification process indicate that the proposed method can achieve minimum profit loss. This method is useful in economic control chart design and can provide guidance for the petrochemical industry.

Keywords petrochemical, PTA, economic control chart design, process monitoring, DE algorithm

Received May 22, 2017; accepted August 23, 2017

Zhi LI, Feng QIAN, Wenli DU, Weimin ZHONG (✉)
Key Laboratory of Advanced Control and Optimization for Chemical Processes, Ministry of Education, East China University of Science and Technology, Shanghai 200237, China
E-mail: wmzhong@ecus.edu.cn

1 Introduction

The petrochemical industry is one of the fundamental industries and provides a variety of raw materials and products for the human society, such as fuel, energy, fertilizer, and fiber. Purified terephthalic acid (PTA) is one of the most important petrochemical products and is a key raw material in the polyester industry (Li et al., 2015; Li et al., 2016). PTA production is a typical petrochemical process which involves heat transfer, mass transfer, momentum transfer, and reactions. The equipment for this process includes pumps, heat exchangers, reactors, distillation column, crystallizers, and tanks. In an industrial plant, homogeneous liquid-phase oxidation of *p*-xylene (PX) with air or molecular oxygen in an acetic acid solvent is the most common method for PTA production. However, the products of the oxidation process contain an impurity, that is, 4-carboxybenzaldehyde (4-CBA), which is harmful to the polyester industry. Thus, a hydropurification process is applied to eliminate 4-CBA. Crude terephthalic acid (CTA) from the oxidation process silo is heated to approximately 273°C and reacts with hydrogen in a fixed-bed reactor with Pd/C catalyst (Azarpour and Zahedi, 2012). In this process, the 4-CBA impurity is reduced from 3000 ppm to less than 25 ppm to achieve the material requirement of the polyester industry. Therefore, the hydropurification process plays an essential role in the industrial PTA production process. In the real industrial PTA process, many disturbances occur, which may lead to process failure, thereby affecting product quality. Although many studies focused on the mechanism of the PTA process, such as reactions, modeling, control, and optimization, only a few studies considered monitoring and fault detection in this process.

With the development of computer science and the application of distributed control system, large amounts of production process historical data are collected and stored. From these data, many data-based process monitoring and fault detection methods have been proposed in recent

years. Statistical process control methods, such as principal component analysis (Lu et al., 2004), partial least squares (Wang and Shi, 2014; Hu et al., 2013), and independent component analysis (Lee et al., 2004), are well-known fault detection methods. Most of these methods use T^2 and SPE statistic as control limits to detect the faults of the process. However, these methods only focus on statistical performance, such as false detection and miss rates. Although the monitoring results exceed the T^2 or SPE control limit, the process can remain in a normal working state for a while or remain unaffected even when the process variables are faulty. The overall profit loss of detection should be considered in process monitoring. Thus, several related studies regarding economic control chart design have been reported. In 1980, Montgomery reported that the design of a control chart from an economic viewpoint has been the focus of considerable attention (Montgomery, 1980). In 1993, Rahim et al. proposed a generalized model for the economic design of x control charts for production systems (Rahim and Banerjee, 1993). Chen et al. (2007) developed an economic design of VSSI control charts for correlated data. In 2011, Chih et al. used the particle swarm optimization (PSO) method for the economic control chart designs (Chih et al., 2011).

In this study, the differential evolution (DE) algorithm is used to develop the economic control chart for a typical petrochemical process. The DE algorithm has been one of the well-known evolution algorithms in the past 20 years and is arguably one of the most powerful stochastic real-parameter optimization algorithms in current use (Das and Suganthan, 2011). Different fault types and process data that contain information on the common faults of the PTA hydropurification process are collected from an exact plant-wide model (Li et al., 2016). A novelty of this study is that the key parameters used to establish the economic control chart are obtained by the optimization algorithm based on the processes and financial data of a real-world continuous chemical process.

The remainder of this paper is organized as follows. Section 2 describes the PTA hydropurification process. Section 3 presents the proposed DE-based economic control chart design. Section 4 analyzes a series of case studies and different types of process faults. Finally, Section 5 draws the conclusions.

2 Process description and fault analysis

2.1 CTA hydropurification process

As previously described, the CTA hydropurification process is a typical petrochemical process. The flowchart of this process is shown in Fig. 1. The solid CTA from the silo of the PX oxidation process has approximately 3000 ppm of 4-CBA. Then, the solid CTA is pumped into five simultaneous preheaters (YR101A-E) with deionized water as the solvent. The temperature of the CTA slurry is gradually increased from room temperature to 273°C by the preheaters. Then, the CTA slurry is injected into the top of the fixed-bed reactor filled with Pd/C catalyst. Another stream, that is, hydrogen, is injected into the top of the fixed-bed reactor. The reaction of 4-CBA in the CTA slurry and hydrogen occurs on the surface of the catalyst. Through this reaction, 4-CBA is converted to *p*-toluic and benzoic acids, which can be isolated by dryers and centrifuges in the subsequent step. The reactions are expressed in Eqs. (1)–(7) (Zhou et al., 2006 a; Zhou et al., 2006 b). The kinetic parameters are shown in Table 1 (Li et al., 2016). After the reaction, the product from the reactor goes into five crystallizers to lower the temperature and progressively reduce the pressure. Then, the products are sent to the dryers and centrifuges. Finally, PTA is obtained with less than 25 ppm 4-CBA content.

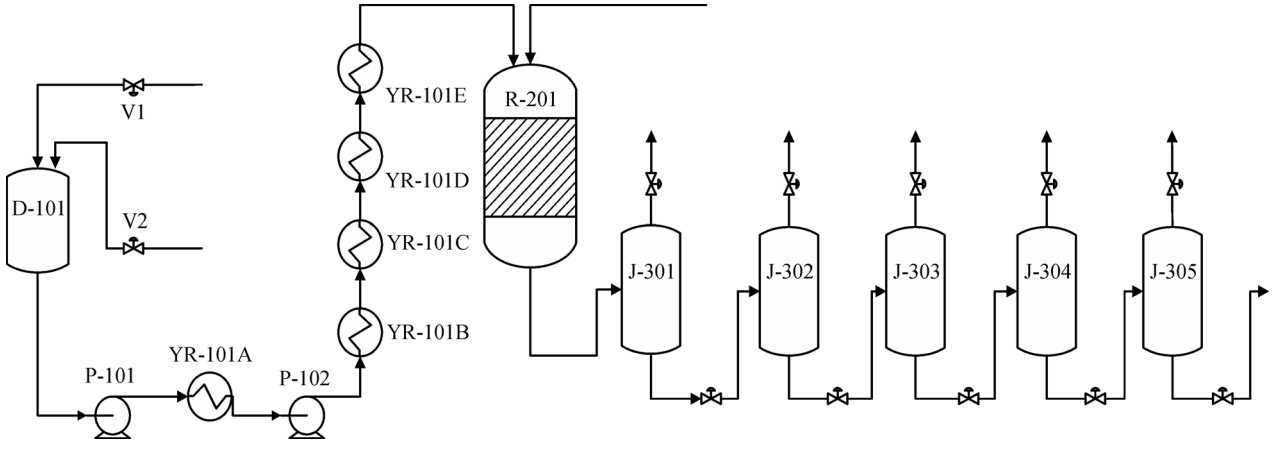

Fig. 1 Flowchart of the CTA hydropurification process

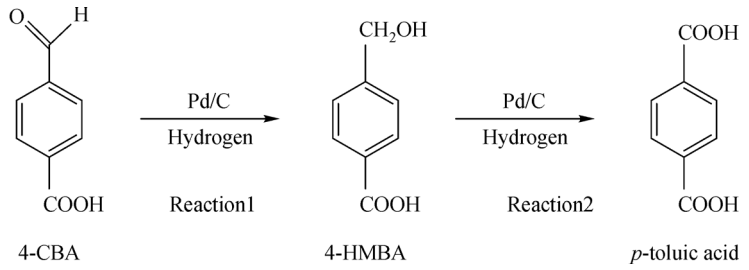

(1)

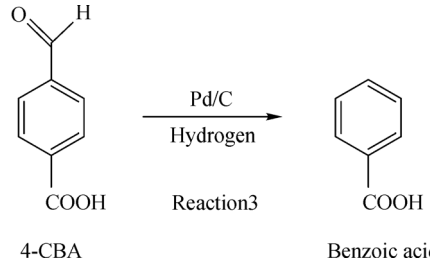

(2)

$$-\frac{\mathrm{d}c_{4-\mathrm{CBA}}}{\mathrm{d}t}=k_{01}e^{-\frac{E1}{RT}}C_{4-\mathrm{CBA}}^{n1}C_{H_2}^{n2} \tag{3}$$

$$\frac{\mathrm{d}c_{4-\mathrm{HMBA}}}{\mathrm{d}t}=k_{01}e^{-\frac{E1}{RT}}C_{4-\mathrm{CBA}}^{n1}C_{H_2}^{n2}-k_{02}e^{-\frac{E2}{RT}}C_{4-\mathrm{HMBA}}^{n3}C_{H_2}^{n4} \tag{4}$$

$$\frac{\mathrm{d}c_{p-\mathrm{Toluic\ acid}}}{\mathrm{d}t}=k_{02}e^{-\frac{E2}{RT}}C_{4-\mathrm{HMBA}}^{n3}C_{H_2}^{n4} \tag{5}$$

$$-\frac{\mathrm{d}c_{4-\mathrm{CBA}}}{\mathrm{d}t}=k_{03}e^{-\frac{E_3}{RT}}C_{4-\mathrm{CBA}}^{n5} \tag{6}$$

$$\frac{\mathrm{d}c_{BA}}{\mathrm{d}t}=k_{03}e^{-\frac{E_3}{RT}}C_{4-\mathrm{CBA}}^{n5} \tag{7}$$

Table 1 Kinetic data of the reactions

Item	Data in this study (Li et al., 2016)
Frequency factor	$k_{01}=0.88$ $k_{02}=0.5971$ $k_{03}=68$
Reaction order	$n_1=0.98,\ n_2=0.26,\ n_3=0.70,$ $n_4=0.60,\ n_5=0.30$
Activation energy	$E_1=18.66\ \mathrm{kJ\cdot mol^{-1}},$ $E_2=28.04\ \mathrm{kJ\cdot mol^{-1}},$ $E_3=724.143\ \mathrm{kJ\cdot mol^{-1}}$

2.2 Analysis of the main faults of the hydropurification process

Different kinds of faults, such as controller, actuator, sensor, and parameter faults, occur in a chemical process. Either of these faults may cause process failure. However, not all of these faults are critical to the plant. Faults occur due to a few major issues in the production process. In the hydropurification process, the most important equipment is the reactor. Thus, the main faults can be categorized into four types. Each of the four main faults is the key factor affecting the process, particularly the reactor.

The first type of fault is reaction temperature. During production, the reaction is sensitive to the temperature, which should be maintained at approximately 273°C. Once the temperature increases, the catalyst may sinter, thereby affecting the efficiency of the reaction. Moreover, the process should be terminated to replace the catalyst. Given that the price of the catalyst is high, the replacement will lead to considerable profit loss. By contrast, when the temperature decreases, the reaction cannot properly work. Therefore, the impurities in the product will be higher than 25 ppm, which will lead to product failure.

The second type of fault is hydrogen flow rate. Hydrogen is the most important reactant in the hydropurification process. Thus, the hydrogen flow rate should be controlled in a certain range. Obviously, hydrogen will be wasted if the flow rate is high. By contrast, the reactant may not completely react if the flow rate is low.

The third type of fault is feed flow rate. The production rate of most chemical plants is fixed during a certain period and is related to the design and operation of the entire plant. Once the production rate is fixed, the operating conditions and plant parameters will be mostly based on the feed flow. In the hydropurification process, the sizes of the preheater, reactor, and crystallizers, as well as the hydrogen flow rate, are designed for the CTA feed flow of 80,000 $\mathrm{kg\cdot h^{-1}}$, and the concentration of the slurry is 29%. When the CTA feed flow is high, the plant cannot handle the extra impurities in the slurry, and the high concentration of the slurry may crush the catalyst bed, thereby causing failure and even an accident. When the CTA feed flow is low, a portion of the production rate is wasted. This phenomenon is called profit loss.

The fourth type of fault is catalyst deactivation. Pd sintering, rapid poisoning by sulfur compounds and other elements, mechanic destruction, corrosion, and fouling are the most common reasons for Pd/C catalyst deactivation. In the hydropurification process, the deactivation time is

approximately one year (Li et al., 2016; Azarpour and Zahedi, 2012). Undoubtedly, catalyst deactivation results in an insufficient reaction. Moreover, catalyst loss is costly.

Table 2 shows the main fault types of the terephthalic acid hydropurification process. The data are collected from the model published in 2015 (Li et al., 2015).

Table 2 Fault types of the terephthalic acid hydropurification process

Fault No.	Fault type
1	CTA feed flow
2	Reaction temperature
3	Hydrogen feed flow
4	Catalyst performance

3 Process monitoring

Only a few key variables and product quality indexes can be manipulated in the CTA hydropurification process, and the data dimension is low. Thus, the common kernel partial least squares (KPLS) method is applied in this study to monitor the four main faults, as well as step and ramp faults. Given that KPLS is not the focus of this study, a brief description of the use of KPLS is provided.

First, the normal working conditions in using the KPLS are developed, which include the following steps:

(1) Data sampling under normal operating conditions;

(2) Standardize the data and ensure that the mean value is equal to zero and the variance is equal to one;

(3) Perform the kernel matrix calculation on the processed data;

(4) Feature space centering;

(5) Calculate the scores of input and output data using the KPLS;

(6) Calculate T^2 of the normal working conditions;

(7) Develop the T^2 control limit based on the sampling method.

Then, the new data are monitored using the developed model, which include the following steps:

(8) Standardize the new sample using the mean value and variance of the normal working data;

(9) Calculate the kernel vector of the new sample;

(10) Centralize the new kernel vector based on step (3);

(11) Calculate the score vector T of the new sampling data;

(12) Calculate the new T^2 control limit;

(13) Compare the new T^2 control limit with that in Step (7); if the new T^2 control limit is exceeded, then the new sample is faulty.

The monitoring results of the four main faults obtained using the KPLS are shown in Fig. 2. The first 400 samples are considered to be in the normal condition. Meanwhile, faults are induced in Sample 401 onward. A total of 5% step and ramp faults of different variables are also considered. In the figure, the red line denotes the control limit, and the blue line denotes the calculated statistic. All of the step fault statistics exceeded the control limit from Sample 401 onward, illustrating that the KPLS is capable of monitoring step faults in the CTA hydropurification process. However, in the ramp tests, the statistics gradually increased after Sample 400 and exceeded the control limit after Sample 500, indicating that the KPLS is unable to deal with slow time-varying process faults. Furthermore, the statistics of the normal working conditions are higher than those of the control limit, and the statistics of the fault conditions are lower than those of the control limit. This finding indicates that false and miss alarms also occur when using the KPLS. False alarms will increase the workload of maintenance inspectors, resulting in increased maintenance costs. Miss alarms will delay the discovery time, a serious situation that may lead to process accidents.

4 Economic control chart design for the CTA hydropurification process

4.1 VSSI-T^2 control chart

In the KPLS or other common monitoring methods, the sampling strategy is fixed when developing the T^2 control chart. In a chemical process, the number of process variables x, which needs to be monitored, is assumed to be $m(m \geqslant 2)$. Vector $X = (x_1, x_2, x_3, \cdots, x_m)$ represents these variables. The mean value of X is $\mu = (\mu_1, \mu_2, \mu_3, \cdots, \mu_m)$, and the covariance matrix is $\sum(m \times m)$. μ_0 and $\sum_0$ are defined as the mean value and covariance matrix under normal conditions, respectively, and n is the sample size.

If μ_0 and $\sum_0$ are known, then the T^2 control chart is calculated using Eq. (8), as follows:

$$T^2 = n(x_i - \mu_0)' \sum\nolimits_0^{-1} (x_i - \mu_0). \tag{8}$$

For the given confidence level $1-\alpha$, the upper control limit $UCL = X^2_{p,\alpha}$ and the lower control limit $LCL = 0$.

If μ_0 and $\sum_0$ are unknown, then UCL and LCL are derived as follows:

$$\begin{cases} UCL = \dfrac{m(n^2-1)}{n(n-m)} F_\alpha(m, n-m) \\ LCL = 0 \end{cases}. \tag{9}$$

Generally, if all of the T^2 statistics are lower than the control limit, then the process is considered to be in the normal condition. However, a small probability of miss and false alarm cases still exists due to statistical compliance with the chi-square distribution. In this study, variable sampling size and interval are considered. This method divides the control chart into three parts: relaxing, tightening, and action regions. In Fig. 3, w is the alarm limit and k is the control limit. The subsequent sampling

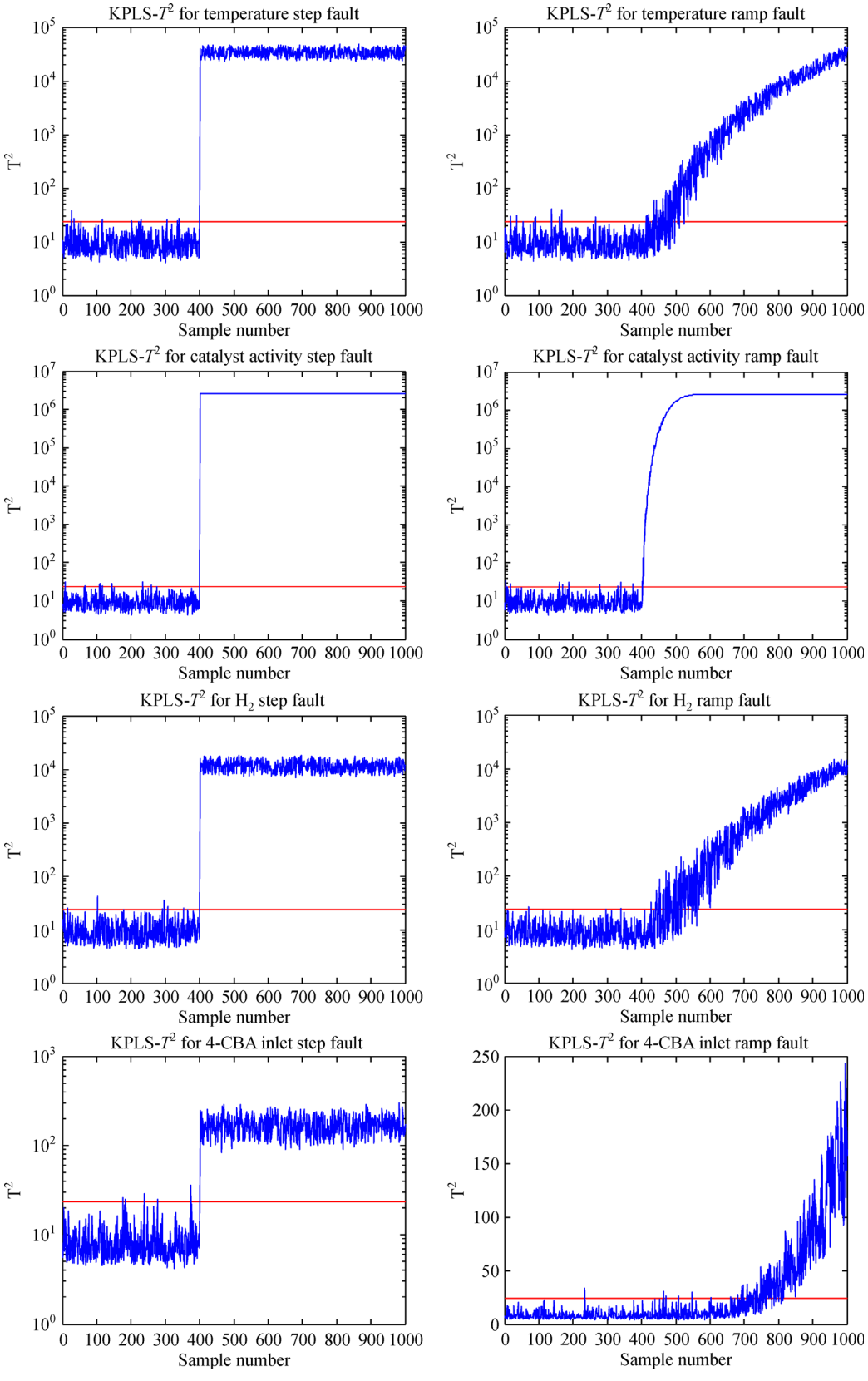

Fig. 2 Monitoring results of the four main faults of the CTA hydropurification process based on the KPLS

strategy is determined based on the position of the last statistic in the control chart. n_1 and n_2 represent two kinds of samples, while (n_1<n_2) and h_1 and h_2 represent two kinds of sampling intervals (h_1<h_2). In the VSSI-T^2 sampling method, the parameters n_1,n_2,h_1,h_2,w,k,m determine the performance of the control chart (Chen et al., 2007).

$$\Big(n(\text{new}),h(\text{new})\Big)=\begin{cases}(n_1,h_1) & 0\leqslant T^2_{\text{new}-1}\leqslant w\\ (n_2,h_2) & w<T^2_{\text{new}-1}\leqslant k\\ \text{fault} & k\leqslant T^2_{\text{new}-1}\end{cases}. \quad (10)$$

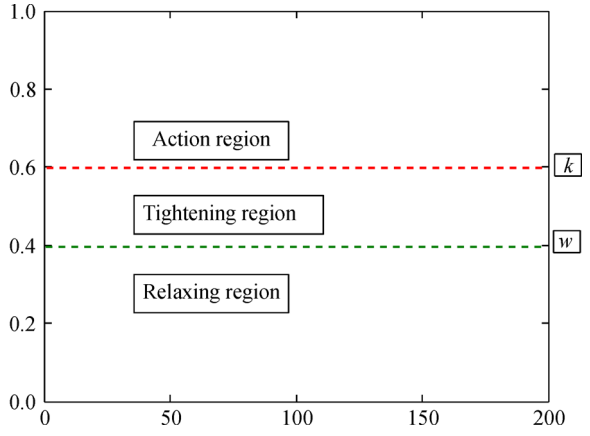

Fig. 3 Relaxing, tightening, and action regions in the VSSI-T^2 control chart

4.2 Economic performance of the control chart

Economic efficiency is one of the most important goals in the chemical production process. The economic control chart is a design method which adopts the optimization strategy to consider cost and quality and minimize quality loss. In this study, the cost model proposed by Costa (Costa, 1993, 1997) is used for the economic design of the $\tilde{X}$ control chart. The three assumptions in this model are as follows.

(1) The process started in the normal condition. In the uncertain future, when affected by a certain factor, the mean vector of the process shifts, the offset δ is represented by the Mahalanobis distance, and the covariance matrix remains unchanged.

$$\delta=\sqrt{(\mu_1-\mu_0)'\sum{}^{-1}(\mu_1-\mu_0)}. \quad (11)$$

(2) When the mean vector shifts, the process changes from normal working conditions to the fault condition, and the process cannot return to the normal condition until detection and maintenance. The occurrence probability of this particular factor follows the λ exponential distribution, and the mean time interval of this fault is $1/\lambda$.

(3) When T_i^2 exceeds the control limit, detection starts.

The key to the economic control chart design is to determine the economic loss function based on the real process. The purpose is to derive a set of parameters that can be used to design the control charts. The cost function is expressed as follows:

$$E(L)=V_0-E(C)/E(T), \quad (12)$$

where V_0 is the profit per hour under normal conditions, $E(C)$ is the mean profit of a specified period, and $E(T)$ is the mean time of this period, which is expressed as follows:

$$E(T)=T_1+T_2+T_3+T_4, \quad (13)$$

where T_1 is the time of the normal working duration, T_2 is the time of the fault working duration, T_3 is the false alarm duration, and T_4 is the time necessary to identify and repair the fault.

Based on the previously presented assumptions, the net profit is calculated as follows:

$$E(C)=V_0\times(1/\lambda)+V_1\times(ATC-1/\lambda)-A_0\times ANF-A_1-C_0\times ANI, \quad (14)$$

where ACT is the average time of the cycle, ANF is the mean false alarm times, ANI is the mean number of sampling points, V_0 is the profit per hour under normal conditions, V_1 is the profit per hour under fault conditions, A_0 is the mean cost of false alarms, A_1 is the mean cost of detection and maintenance, C_0 is the cost of a single sample, T_F is the detection time of false alarms, and T_R is the time required for fault location and maintenance.

4.3 Economic control chart design parameter solution based on the DE algorithm

As introduced in the previous section, the economic design of the $\tilde{X}$ control chart is an optimization problem with constraints that contain continuous and discrete decision variables. The penalty method is one of the common methods used to transform a constrained problem to an unconstrained optimization problem. Through this, an unconstrained optimization method can be used to minimize a single objective problem.

The simplified programming model of the control chart is based on the model previously developed by Chih et al. (2011). The assumption is that the cost model of the control chart is normally distributed.

$$\begin{aligned}&\min && E(L)(n_1,n_2,h_1,h_2,w,k,\delta)\\ &\text{s.t.} && 0<n_1<n_2\\ &&& 0<h_2<h_1\\ &&& 0<w<k\end{aligned} \quad (15)$$

After simplification, the problem could be more efficiently solved. The penalty function can be found in

Reference (Li et al., 2016). In this study, the DE algorithm is used to solve the single-objective optimization problem. A step-by-step framework for solving this problem using the DE algorithm is proposed in Table 3. This framework of the DE algorithm is well-known and widely used in many optimization areas. All of the required codes have been written in MATLAB R2010b.

The parameters of the algorithm are as follows: $F = 0.4$; $CR = 0.9$; $eps = 10^{-6}$; the population size is 30, and the maximum iterations are 1000. Moreover, $\lambda = 0.01$, $\alpha = 0.5$, $1-\beta = 0.9$, $h = 1$, $n = 10$, and $\delta^2 = 2$. The process variables are shown in Table 4.

Table 3 Framework of the DE algorithm

Population initialization: Generate n-dimensional vectors randomly, and the number of vectors is given as NP.
For continuous variables:
$x_{ij}(0) = x_{ij}^L + rand(0,1)(x_{ij}^U - x_{ij}^L)$
For discrete variables:
$y_{ij}(0) = y_{ij}^L + \lfloor rand(0,1)(y_{ij}^U - y_{ij}^L) \rfloor$
Objective function evaluation.
Evolution loop:
If do not meet the termination condition
For each vector at current generation
Do mutation operation
$h_{ij}(g) = x_{p1} + F(x_{p2j} - x_{p3j})$
End
For each vector at current generation
Do crossover operation

$$v_{ij}(g+1) = \begin{cases} h_{ij}(g), rand(0,1) \leqslant CR \text{ or } j = rand(1,n) \\ x_{ij}(g), rand(0,1) \leqslant CR \text{ or } j \neq rand(1,n) \end{cases}$$

$CR \in [0,1]$
Evaluate the objective value
End
For each vector at current generation
Do selection operation

$$x_i(g+1) = \begin{cases} v_i(g+1), f\left(v_i(g+1)\right) < f\left(x_i(g)\right) \\ v_i(g), f\left(v_i(g+1)\right) \geqslant f\left(x_i(g)\right) \end{cases}$$

End
End If
Output optimization result.

The profit loss determined using the GA, PSO, and DE algorithms is shown in Table 5. The DE algorithm derives the minimum profit loss. The iteration process of the three methods is shown in Fig. 4, where the DE algorithm is evidently the fastest method. The profit loss of the four main faults determined using different parameters of the T^2 and VSSI-T^2 control charts are shown in Table 6. The sampling numbers n_1 andn_2, sampling intervals h_1 and h_2, upper limit w, and lower limit k are also listed in Table 6. When δ = 0.5, 1, 1.5, 2, VSSI-T^2 control chart always obtains the minimum $E(L)$. This finding indicates that the parameters of the VSSI-T^2 control chart calculated by the DE algorithm can significantly improve the economy of the control chart.

5 Conclusions

In this study, an economic control chart design method is proposed for a typical petrochemical process monitoring. Most of the traditional control charts mainly focus on false detection and miss rates, and only a few studies focus on the economic problems of the control chart. A VSSI-T^2 control chart is developed based on variable sampling size and interval. Afterward, a profit loss model is established based on the real industrial CTA hydropurification process. Then, the problem of solving VSSI-T^2 parameters is transformed into an optimization problem considering cost and profit. Subsequently, the DE algorithm is used to solve the optimization problem. Results show that the proposed control chart can achieve the minimum profit loss for CTA hydropurification process monitoring.

In future works, the online application of this method

Table 4 Parameters used in economic control chart design for the CTA hydropurification process

Variables	Fault 1	Fault 2	Fault 3	Fault 4
T_f (h)	0.1	2	0.25	0.2
T_R (h)	0.5	10	1	0.8
V_0 (10,000 CNY)	80	80	80	80
V_1 (10,000 CNY)	52	57	72	78
A_1 (10,000 CNY)	10	60	5	1
A_0 (10,000 CNY)	0.2	50	0.2	0.2
C_0 (10,000 CNY)	1	7	0.5	0.3

Table 5 The expected profit loss of the economic control chart using GA/PSO/DE (CNY)

Fault No.	GA	PSO	DE
1	5824.0828	5727.3059	5726.2084
2	6423.8950	6398.5473	6358.7028
3	283.6723	280.5963	277.1632
4	121.0571	120.8943	118.838

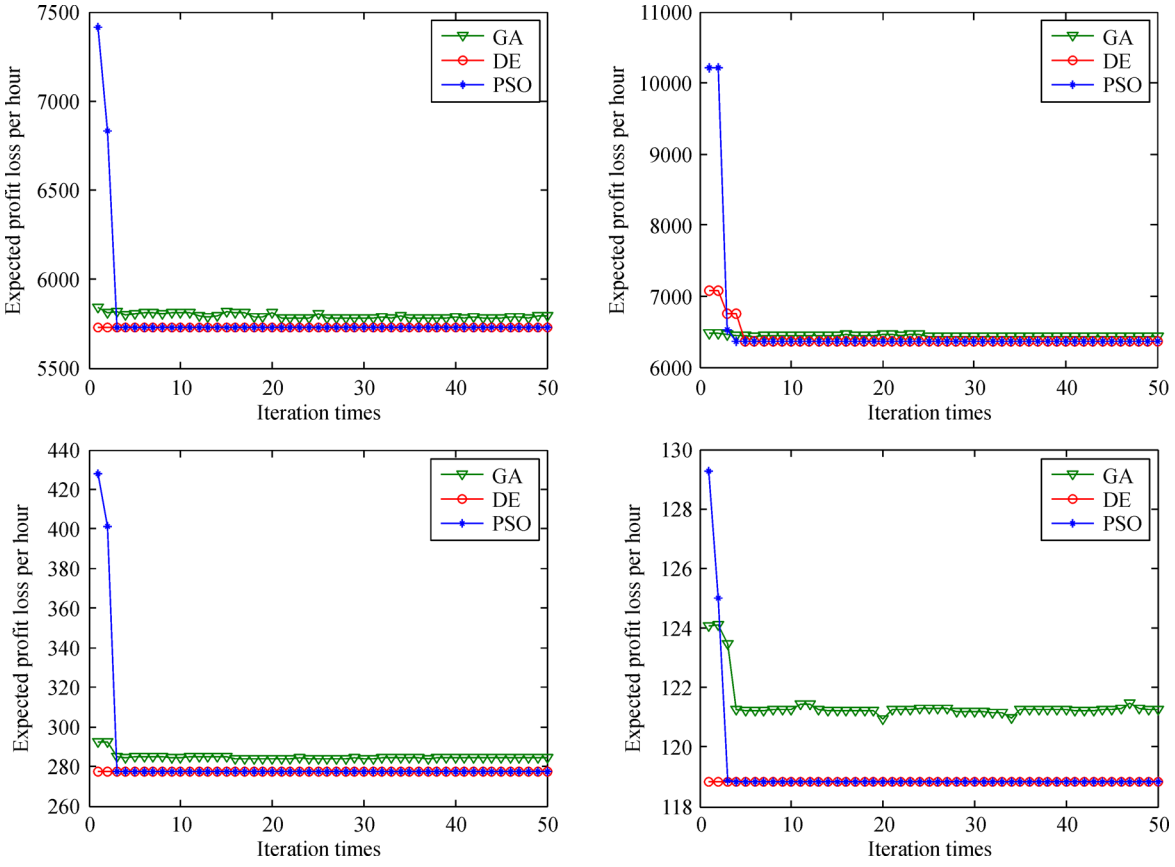

Fig. 4 Control chart parameter optimization process of three algorithms for four step faults

Table 6 Comparison results of T^2 and VSSI-T^2 with different parameters

Fault	δ^2	Control chart type	$E(L)$ /(CNY·h^{-1})	Sampling number		Sampling interval		Control limit	
				n_1	n_2	h_1	h_2	w	k
1	0.5	VSSI-T^2	5747.019	15	18	1.51	1.73	12.451	19.643
		T^2	5750.376	17		1.67		18.5471	
	1	VSSI-T^2	5742.898	10	16	1.21	1.46	17.245	21.374
		T^2	5745.214	14		1.33		20.3896	
	1.5	VSSI-T^2	5732.445	9	14	0.94	1.25	19.147	23.879
		T^2	5735.452	12		1.17		22.5254	
	2	VSSI-T^2	5729.324	8	11	0.69	1.11	21.574	25.771
		T^2	5731.208	10		1		23.6243	
2	0.5	VSSI-T^2	126.430	16	19	1.47	1.62	12.412	19.319
		T^2	127.958	17		1.67		18.5471	
	1	VSSI-T^2	123.745	11	16	1.19	1.44	18.247	21.646
		T^2	125.774	14		1.33		20.4732	
	1.5	VSSI-T^2	120.524	10	14	0.96	1.23	20.854	23.713
		T^2	121.221	12		1.17		22.5254	
	2	VSSI-T^2	6358.703	8	12	0.81	1.04	21.946	25.174
		T^2	119.214	10		1		23.6243	

(*Continued*)

Fault	δ^2	Control chart type	$E(L)$ /(CNY·h^{-1})	Sampling number		Sampling interval		Control limit	
				n_1	n_2	h_1	h_2	w	k
3	0.5	VSSI-T^2	126.430	15	19	1.46	1.79	15.342	20.853
		T^2	127.958	17		1.67		18.5471	
	1	VSSI-T^2	123.745	13	15	1.12	1.54	18.419	22.168
		T^2	125.774	14		1.33		20.3896	
	1.5	VSSI-T^2	120.524	9	13	1.01	1.37	20.315	24.954
		T^2	121.221	12		1.17		22.5254	
	2	VSSI-T^2	118.838	8	12	0.88	1.26	21.747	25.642
		T^2	119.214	10		1		23.6243	
4	0.5	VSSI-T^2	126.430	15	19	1.36	1.81	13.641	19.522
		T^2	127.958	17		1.67		18.5471	
	1	VSSI-T^2	123.745	12	15	1.20	1.47	18.957	22.156
		T^2	125.774	14		1.33		20.3896	
	1.5	VSSI-T^2	120.524	10	13	1.01	1.36	19.485	23.449
		T^2	121.221	12		1.17		22.5254	
	2	VSSI-T^2	118.838	8	12	0.85	1.17	21.032	25.696
		T^2	119.214	10		1		23.6243	

will be investigated, including data coordination in the financial, planning, scheduling, operating, and selling departments, as well as the effect of process failure and unplanned termination on the value chain of the entire petrochemical enterprise.

Acknowledgements This work was supported by the National Natural Science Foundation of China (61422303, 21376077) and Fundamental Research Funds for Central Universities.

References

Azarpour A, Zahedi G (2012). Performance analysis of crude terephthalic acid hydropurification in an industrial trickle-bed reactor experiencing catalyst deactivation. Chemical Engineering Journal, 209: 180–193

Chen Y K, Hsieh K L, Chang C C (2007). Economic design of the VSSI control charts for correlated data. International Journal of Production Economics, 107(2): 528–539

Chih M, Yeh L L, Li F C (2011). Particle swarm optimization for the economic and economic statistical designs of the control chart. Applied Soft Computing, 11(8): 5053–5067

Costa A F B (1993). Joint economic design of $\bar{X}$ and R control charts for processes subject to two independent assignable causes. IIE Transactions, 25(6): 27–33

Costa A F B (1997). Chart with variable sample size and sampling interval. Journal of Quality Technology, 29(2): 197–204

Das S, Suganthan P N (2011). Differential evolution: a survey of the state-of-the-art. IEEE Transactions on Evolutionary Computation, 15 (1): 4–31

Hu Y, Ma H, Shi H (2013). Enhanced batch process monitoring using just-in-time-learning based kernel partial least squares. Chemometrics and Intelligent Laboratory Systems, 123: 15–27

Lee J M, Yoo C, Lee I B (2004). Statistical process monitoring with independent component analysis. Journal of Process Control, 14(5): 467–485

Li Z, Zhong W, Liu Y, Luo N, Qian F (2015). Dynamic modeling and control of industrial crude terephthalic acid hydropurification process. Korean Journal of Chemical Engineering, 32(4): 597–608

Li Z, Zhong W, Wang X, Luo N, Qian F (2016). Control structure design of an industrial crude terephthalic acid hydropurification process with catalyst deactivation. Computers & Chemical Engineering, 88: 1–12

Lu N, Gao F, Yang Y, Wang F (2004). PCA-based modeling and on-line monitoring strategy for uneven-length batch processes. Industrial & Engineering Chemistry Research, 43(13): 3343–3352

Montgomery D C (1980). The economic design of control charts: a review and literature survey. Journal of Quality Technology, 12(2): 75–87

Rahim M A, Banerjee P K (1993). A generalized model for the economic design of xcontrol charts for production systems with increasing failure rate and early replacement. Naval Research Logistics, 40(6): 787–809

Wang L, Shi H (2014). Improved kernel PLS-based fault detection approach for nonlinear chemical processes. Chinese Journal of Chemical Engineering, 22(6): 657–663

Zhou J, Zhang T, Sui Z (2006 a). Hydropurification of terephthalic acid over Pd/C I. thermodynamcis and feature analysis. Journal of East China University of Science and Technology, 32(5): 374–380

Zhou J, Zhang T, Sui Z (2006 b). Hydropurification of terephthalic acid over Pd/C II. apparent kinetics of 4-CBA hydrogenation on catalysts of different sizes. Journal of East China University of Science and Technology, 32(5): 503–507